

# Integral bHLH Factor Regulation of Cell Cycle Exit and RGC Differentiation

Kate A. Maurer,<sup>1</sup> Angelica Kowalchuk,<sup>2</sup> Farnaz Shoja-Taheri,<sup>2</sup> and Nadean L. Brown <sup>1,2\*</sup>

<sup>1</sup>Division of Developmental Biology, Cincinnati Children's Hospital Research Foundation, Cincinnati, Ohio

<sup>2</sup>Department of Cell Biology and Human Anatomy, University of California Davis School of Medicine, Davis, California

**Background:** In the developing mouse embryo, the bHLH transcription factor *Neurog2* is transiently expressed by retinal progenitor cells and required for the initial wave of neurogenesis. Remarkably, another bHLH factor, *Ascl1*, normally not present in the embryonic *Neurog2* retinal lineage, can rescue the temporal phenotypes of *Neurog2* mutants. **Results:** Here we show that *Neurog2* simultaneously promotes terminal cell cycle exit and retinal ganglion cell differentiation, using mitotic window labeling and integrating these results with retinal marker quantifications. We also analyzed the transcriptomes of E12.5 GFP-expressing cells from *Neurog2*<sup>GFP/+</sup>, *Neurog2*<sup>GFP/GFP</sup>, and *Neurog2*<sup>Ascl1KI/GFP</sup> eyes, and validated the most significantly affected genes using qPCR assays. **Conclusions:** Our data support the hypothesis that *Neurog2* acts at the top of a retinal bHLH transcription factor hierarchy. The combined expression levels of these downstream factors are sufficiently induced by ectopic *Ascl1* to restore RGC genesis, highlighting the robustness of this gene network during retinal ganglion cell neurogenesis. *Developmental Dynamics* 247:965–975, 2018. © 2018 Wiley Periodicals, Inc.

**Key words:** *Neurog2*; *Atoh7*; *Ascl1*; retinal ganglion cell; neurogenesis; bHLH factor

Submitted 20 March 2018; First Decision 5 May 2018; Accepted 5 May 2018; Published online 17 May 2018

## INTRODUCTION

In the vertebrate retina, seven neuronal and glial cell classes arise from a common pool of retinal progenitor cells (RPCs) in a highly ordered and partially overlapping sequence (Young, 1985; Turner and Cepko, 1987; Turner et al., 1990; Rapaport et al., 2004). The RPC population expands through continuous rounds of mitotic cell division, which must be integrated with tissue morphogenesis and cell fate determination. The timing of the terminal S-phase (or birthdate) of an RPC strongly influences its postmitotic identity. Retinal neurogenesis initiates centrally and expands outward toward the periphery (Prada et al., 1991; Hu and Easter, 1999; McCabe et al., 1999). In mice, the first wave of neurogenesis begins on embryonic day (E)11.0 and is complete by E13.5 (Sidman, 1961; Hufnagel et al., 2010). Since retinal ganglion cells (RGCs) are the first cell class to differentiate in all vertebrate eyes, their formation is synonymous with the initial wave of neurogenesis.

The onset of ganglion cell formation is characterized by activation of the basic helix-loop-helix (bHLH) transcription factor

*Atoh7* in newly postmitotic RPCs. Although *Atoh7*-expressing cells give rise to all seven major cell classes (Feng et al., 2010; Brzezinski et al., 2012), *Atoh7* bestows competence to a subset of these cells to develop as RGC neurons. The complete absence of RGCs and optic nerves in *Atoh7*-mutant mice illustrates its importance (Brown et al., 2001; Wang et al., 2001). However, downstream of *Atoh7*, the transcription factors *Pou4f2* and *Isl1* are essential to lock in the RGC differentiation program (Mu et al., 2008; Pan et al., 2008; Li et al., 2014; Wu et al., 2015). In the absence of either gene, RGCs are specified but subsequently undergo significant apoptosis (65%–80%) prior to birth (Gan et al., 1996; Gan et al., 1999; Mu et al., 2008; Pan et al., 2008). *Pou4f2* and *Isl1* double-mutant retinas have an even greater loss of RGCs (>95%), highlighting their synergistic relationship (Pan et al., 2008; Li et al., 2014; Wu et al., 2015). *Pou4f1*, *Myt1*, *Ebf3*, *Onecut1*, and *Onecut2* act either in parallel or downstream of *Pou4f2* and *Isl1* during RGC genesis (Erkman et al., 1996; Mu et al., 2008; Jin et al., 2010; Wu et al., 2012; Shi et al., 2013; Gao et al., 2014). However, a better understanding of the regulatory relationships among these genes is still lacking.

Other bHLH proneural factors are also active during retinogenesis. Indeed, *Neurog2* initiates retinal expression in mice at E11.0 within a subset of mitotic RPCs, including those at the leading edge of neurogenesis (Yan et al., 2001; Ma and Wang, 2006; Hufnagel et al., 2010; Brzezinski et al., 2011). In these RPCs, *Neurog2* directly activates *Atoh7* transcription through an evolutionarily

Dr. Maurer's present address is Medpace Central Laboratories Cincinnati, Ohio

Dr. Shoja-Taheri's present address is Department of Biomedical Engineering Emory University, Atlanta, Georgia  
Additional supporting information may be found online in the Supporting Information section at the end of the article.

Grant sponsor: National Eye Institute; Grant numbers: EY013612, T32 EY015387.

\*Correspondence to: Nadean L. Brown, Department of Cell Biology and Human Anatomy, University of California, Davis, Room 4407A Tupper Hall, Davis, CA 95616. E-mail: nlbrown@ucdavis.edu.

Article is online at: <http://onlinelibrary.wiley.com/doi/10.1002/dvdy.24638/abstract>

© 2018 Wiley Periodicals, Inc.

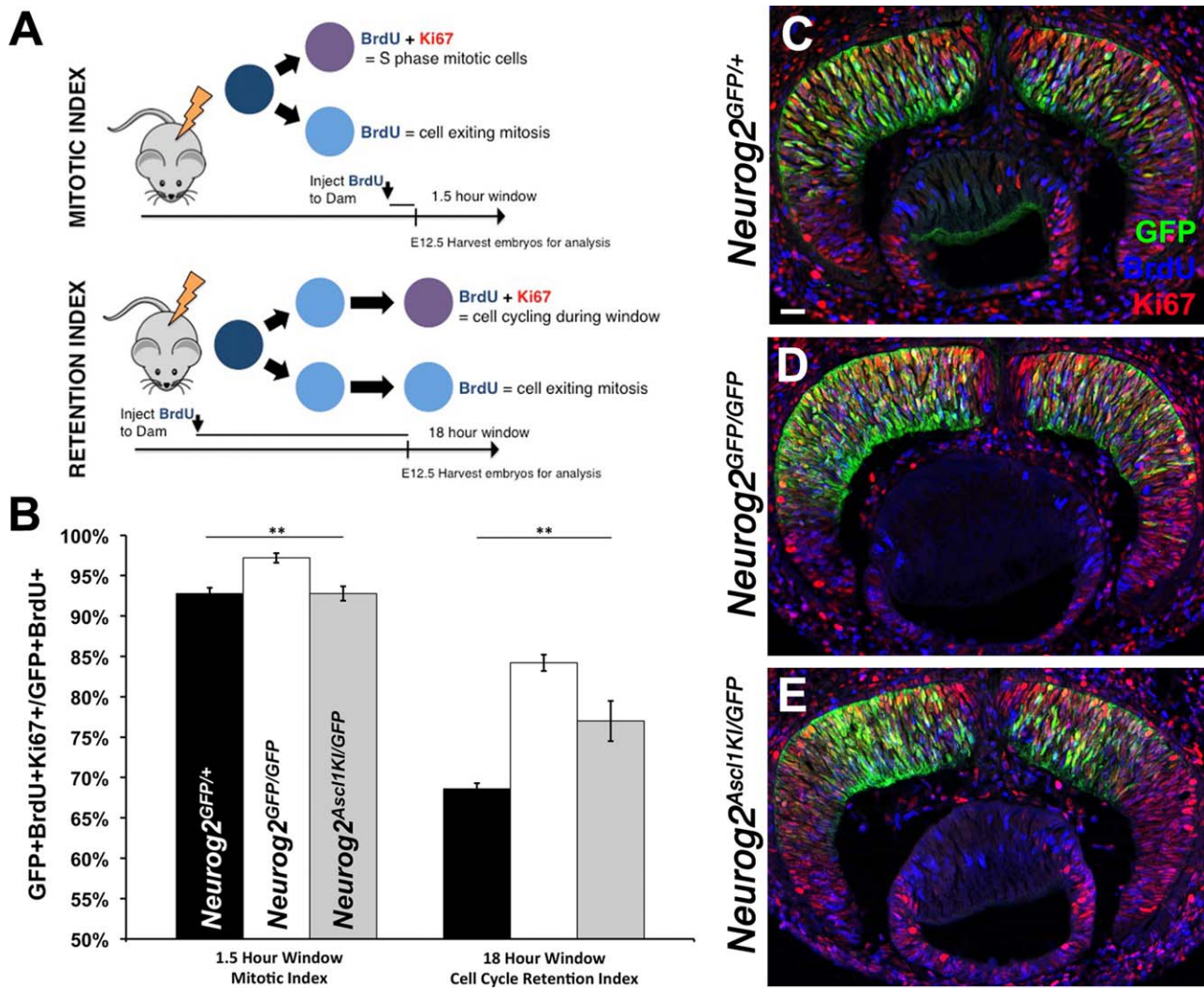


**Fig. 1.** *Neurog2* is required for retinal progenitor cell cycle exit. **A:** Experimental strategy to label RPCs with BrdU for 1.5 hr or 18 hr prior to embryo harvest at E12.0. **B:** Percentages of *Neurog2* lineage cells (GFP+) in the cell cycle. There was a significant increase in mitotic RPCs in *Neurog2*<sup>GFP/GFP</sup> retinas, which was more apparent with a longer labeling window. *Ascl1* recombined into the *Neurog2* locus rescued this phenotype. **C–E:** Representative triple-labeled retinal images for *Neurog2*<sup>GFP/+</sup>, *Neurog2*<sup>GFP/GFP</sup>, and *Neurog2*<sup>Ascl1KI/GFP</sup> embryos after 18-hr BrdU labeling. A one-way ANOVA plus Tukey's post hoc test was used to determine *P* values. \*\* *P* ≤ 0.01; error bars = SEM; n ≥ 3 embryos/genotype; apical is up. Scale bar = 50 μm.

conserved E-box in the primary *Atoh7* retinal enhancer (Riesenberg et al., 2009; Skowronska-Krawczyk et al., 2009). In the absence of *Neurog2*, *Atoh7* expression is delayed along with the advancement of *Pou4f2*+ RGCs (Hufnagel et al., 2010). Another bHLH factor, *Ascl1*, is also expressed by a cohort of proliferating RPCs, beginning at E12.5 (Jasani and Reh, 1996; Brzezinski et al., 2011). Despite partially overlapping expression domains in the prenatal retina, *Neurog2* and *Ascl1* demarcate distinct lineages (Brzezinski et al., 2011). Thus, it was unexpected that misexpression of *Ascl1* in the *Neurog2* lineage rescued *Atoh7* expression and the wave of RGC neurogenesis (Hufnagel et al., 2010). One explanation is that *Neurog2* and *Ascl1* are largely expressed by proliferating RPCs and, thus, share a common set of downstream targets in the retina. (Jasani and Reh, 1996; Yan et al., 2001; Ma and Wang, 2006). Alternatively, the presence of multiple bHLH factors, which include *Neurod1*, *Neurod4/Math3*, and *Olig2*, endows the RGC gene network with sufficient redundancy for the establishment of functional optic nerves. To distinguish among

these possibilities, we used transcriptomics and gene expression analyses to identify genes that require *Neurog2* for their expression but are also up-regulated upon *Ascl1* rescue of RGC development.

## RESULTS

### *Neurog2* Regulation of Cell Cycle Exit

We hypothesized that *Neurog2* must normally regulate some aspect of cell cycle exit because the percentages of both actively mitotic and apoptotic RPCs did not differ among *Neurog2*<sup>GFP/+</sup> (control), *Neurog2*<sup>GFP/GFP</sup> (mutant), and *Neurog2*<sup>Ascl1KI/GFP</sup> (rescue) embryos (Hufnagel et al., 2010). To test this idea, we performed a BrdU window labeling on embryos of all three genotypes (Repka and Adler, 1992). A single injection of BrdU was given intradermally to pregnant dams at either 1.5 or 18 hr prior to sacrifice at E12.0 (Fig. 1A). RPCs in terminal S-phase at



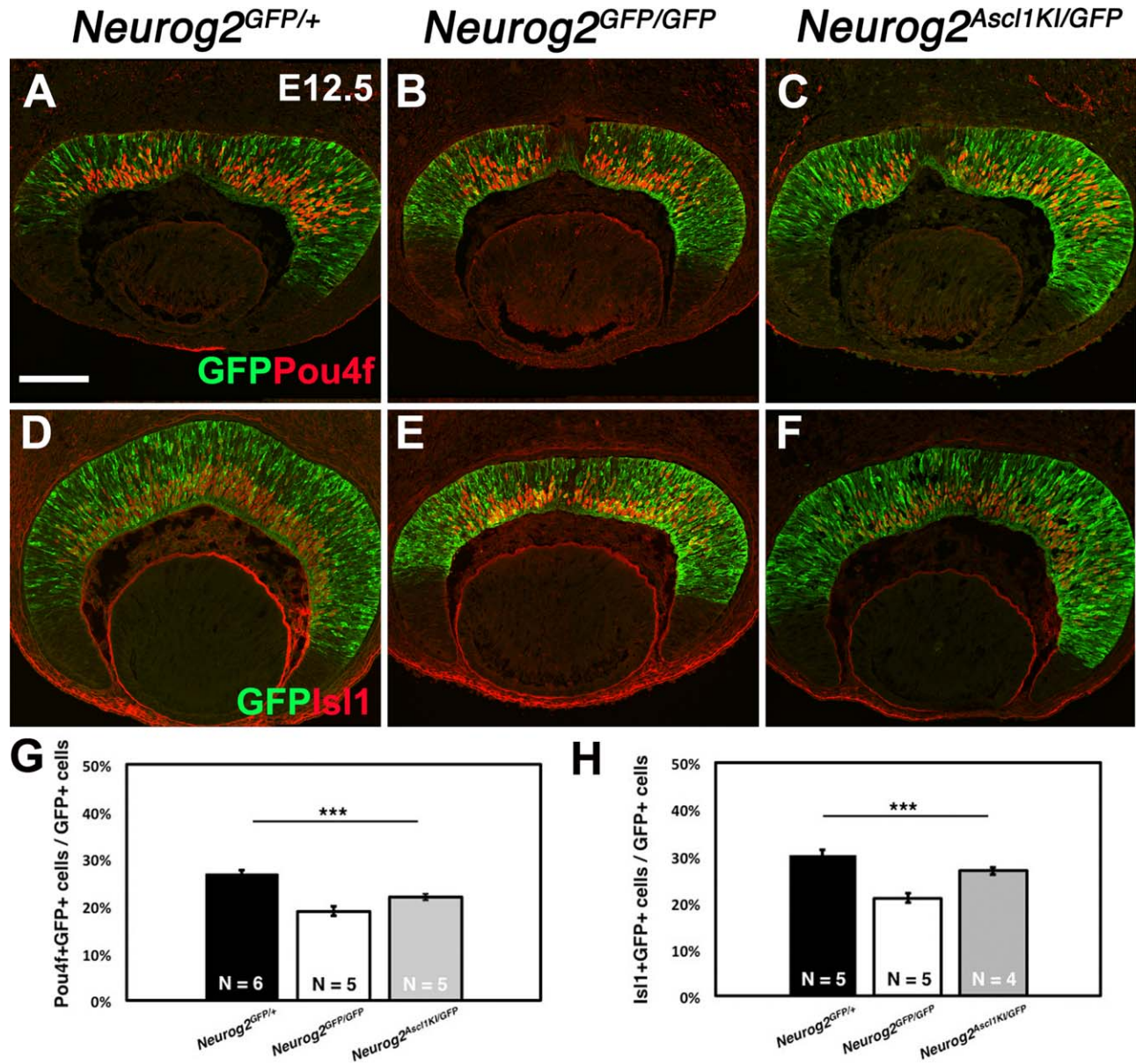


**Fig. 2.** The impact of *Neurog2* loss on RGC differentiation. **A–C,G:** E12.5 Pou4f+RGCs in the *Neurog2<sup>GFP</sup>* lineage are significantly reduced in *Neurog2* mutants but rescued by *Ascl1* misexpression in the *Neurog2* locus. **D–F,H:** E12.5 Isl1+ cells (most of which are RGCs) are analogously reduced in *Neurog2* mutants and rescued by *Ascl1*. A one-way ANOVA plus Bonferroni post hoc test were used to determine *P* values. \*\*\*  $P \leq 0.001$ ; error bars = SEM; apical retina is up;  $n \geq 3$  embryos/genotype. Scale bar = 100  $\mu\text{m}$ .

the time of injection retain BrdU label indefinitely, whereas mitotic RPCs dilute BrdU in subsequent rounds of mitosis. The short window provided a baseline RPC mitotic index, with the long window chosen, based on average RPC cell cycle length at this developmental stage (Alexiades and Cepko, 1996). Retinal sections were co-labeled for BrdU, Ki67, and GFP (to mark the *Neurog2* lineage). We then quantified the percentage of GFP+RPCs that remained mitotic (BrdU+Ki67+) vs. those that exited the cell cycle (BrdU+Ki67-) (Chenn and Walsh, 2002; Kee et al., 2002; Pei et al., 2011). In the short window, there was a significant increase in mitotic RPCs in *Neurog2<sup>GFP/GFP</sup>* retinas compared to *Neurog2<sup>GFP/+</sup>* or *Neurog2<sup>Ascl1KI/GFP</sup>* (Fig. 1B). This increase was more pronounced in the longer time frame, but *Ascl1* provided full rescue during both labeling windows

(Fig. 2B–D). Interestingly, this outcome is not the same as ectopic expression of *Ascl1* in the *Atoh7* lineage. In that gene-replacement mouse, both cell cycle exit and RGC differentiation were blocked, and the *Atoh7<sup>Ascl1KI/+</sup>* RPCs uniquely underwent extra rounds of mitosis (Hufnagel et al., 2013). Although the phenotypes of *Atoh7<sup>Ascl1KI/+</sup>* and *Neurog2<sup>Ascl1KI/GFP</sup>* mice differed, in both situations ectopic *Ascl1* expression induced cell cycle progression.

### *Neurog2* Regulation of RGC Genesis

We next wished to correlate the window-labeling findings with the progress of RGC differentiation. The RGC markers Pou4f and Isl1 had abnormal expression patterns in *Neurog2<sup>GFP/GFP</sup>*

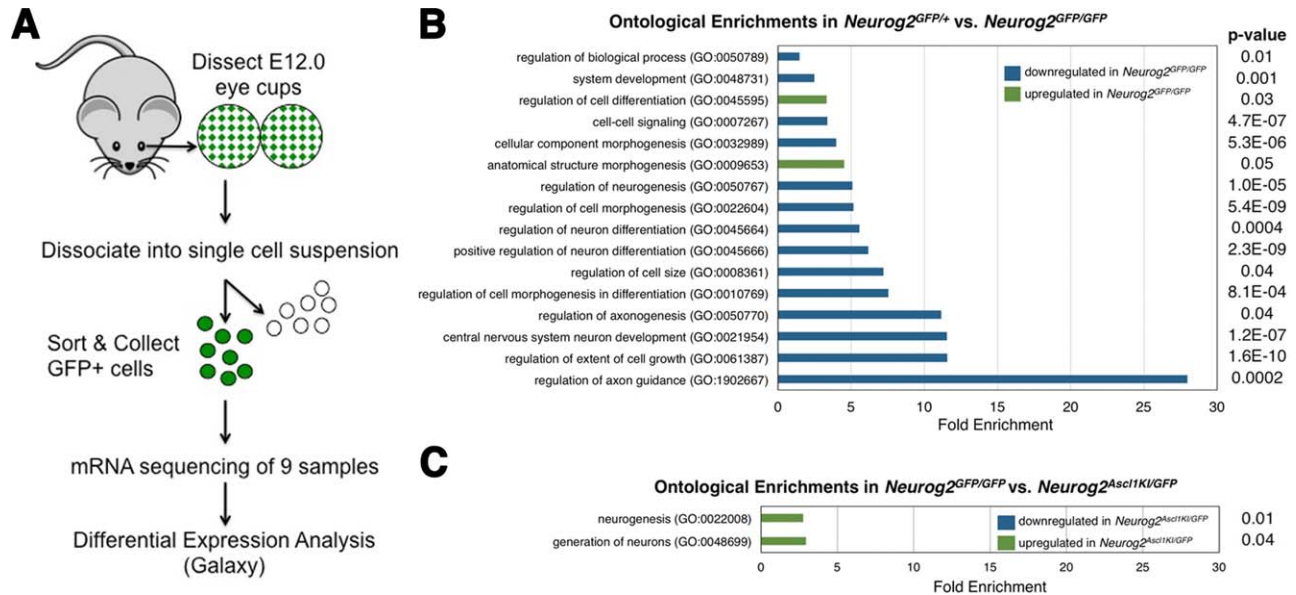


**Fig. 3.** High-throughput analysis of transcriptional changes in E12.5 *Neurog2*-GFP+ RPCs among three genotypes. **A:** Workflow diagram of optic cup collection, dissociation, and flow-sorting of GFP+;7-AAD-neg populations from *Neurog2*<sup>GFP/+</sup>, *Neurog2*<sup>GFP/GFP</sup>, and *Neurog2*<sup>Ascl1KI/GFP</sup> embryos, followed by RNA-seq analyses. **B, C:** Gene ontology analyses among the genotypes, with statistically significant functional groups ranked by fold enrichment. Blue bars indicate GO categories with significant down-regulated gene expression; green bars denote categories with significant up-regulated expression.

mutants, which were restored in *Neurog2*<sup>Ascl1KI/GFP</sup> eyes (Hufnagel et al., 2010). However, these outcomes were not quantified. Using specific pan-Pou4f or Isl1 antibodies, we labeled E12.5 retinal sections, along with anti-GFP (Fig. 2A–F), to determine the percentages of marker+GFP+ per total GFP+ cells (Fig. 2G,H). Overall, we noted a reduction of Pou4f+ (8%) or Isl1+ (9%) cells in *Neurog2*<sup>GFP/GFP</sup> retinas compared to *Neurog2*<sup>GFP/+</sup>. There was also a rebound of Pou4f+ (3%) or Isl1+ (6%) cells in *Neurog2*<sup>Ascl1KI/GFP</sup> eyes as compared to mutants. These shifts in nascent RGCs complemented the increased mitotic index found in *Neurog2*<sup>GFP/GFP</sup> eyes (4%) and its return to a nearly wild-type rate in *Neurog2*<sup>Ascl1KI/GFP</sup> eyes (4%) (Fig. 1B, short window). Thus, we concluded that *Neurog2* normally regulates both the terminal cell cycle exit and differentiation of early RGC neurons.

### Genes Expressed Downstream of *Neurog2*

To generate an unbiased view of gene expression during the initial wave of neurogenesis, we compared the retinal transcriptomes of E12.5 *Neurog2*<sup>GFP/+</sup>, *Neurog2*<sup>GFP/GFP</sup>, and *Neurog2*<sup>Ascl1KI/GFP</sup> embryos. Because *Neurog2* heterozygotes are phenotypically indistinguishable from wild-types (Hufnagel et al., 2010), we took advantage of the live reporter in *Neurog2*<sup>GFP/+</sup>, *Neurog2*<sup>GFP/GFP</sup>, and *Neurog2*<sup>Ascl1KI/GFP</sup> to isolate GFP+ RPCs by flow cytometry, using the 7AAD dye to gate out any dying cells (Fig. 3A). An average of 22,000 GFP+7AAD-RPCs were used for total RNA isolations from *Neurog2*<sup>GFP/+</sup> (n = 14), *Neurog2*<sup>GFP/GFP</sup> (n = 6), and *Neurog2*<sup>Ascl1KI/GFP</sup> (n = 14) embryos (see Experimental Procedures for details). The resulting cDNA libraries then underwent next-gen sequencing. We used the Galaxy bioinformatics platform (www.usegalaxy.org) to analyze the resulting data sets (n = 3 biologic replicates/genotype). First, we compared *Neurog2*<sup>GFP/+</sup> and *Neurog2*<sup>GFP/GFP</sup> transcriptomes, and then we compared the *Neurog2*<sup>GFP/GFP</sup> and *Neurog2*<sup>Ascl1KI/GFP</sup> transcriptomes (Figs. 3 and 4). Genes whose

transcript levels significantly differed ( $Q \leq 0.05$ ) were classified further by ontology using the PANTHER program (www.geneontology.org). Those biologic processes with statistically valid changes in fold enrichment ( $P \leq 0.05$ ) were then graphed relative to one another (Fig. 3B,C). Groups associated with neurogenesis, neuronal differentiation, and axon guidance were most highly down-regulated in *Neurog2*<sup>GFP/GFP</sup> retinal cells, whereas smaller groups of genes regulating differentiation, or acting during morphogenesis, were up-regulated (Fig. 3B). Remarkably, just two ontologic groups, neurogenesis and generation of neurons, were up-regulated in *Neurog2*<sup>Ascl1KI/GFP</sup> eyes, with none of the groups listed in Figure 3B undergoing significant down-regulation (Fig. 3C).

As a proof of principle, we expected to see the absence of *Neurog2* transcripts in the *Neurog2*<sup>GFP/GFP</sup> and *Neurog2*<sup>Ascl1KI/GFP</sup> transcriptomes. Instead, the *Neurog2* RPKM (reads per kilobase of transcript, per million mapped reads) values for both genotypes were higher than for heterozygotes (Fig. 4). To explain this puzzling result, we visualized the distribution of the sequence reads at the *Neurog2* locus for all three genotypes, using the IGV program (Fig. 5A). The *Neurog2* gene has two exons and one intron, with the open reading frame (ORF) located in the second exon (Gradwohl et al., 1996; Sommer et al., 1996; Fode et al., 1998). In both gene-replacement strategies, *Neurog2* protein-coding sequences were swapped out for either a GFP or *Ascl1* cDNA, thereby creating functionally null alleles that retained *Neurog2* 5' and 3' UTR sequences (Fode et al., 2000; Seibt et al., 2003). Our aligned sequence reads highlighted a bias among all three genotypes for the *Neurog2* UTRs. However, for both mutant alleles, no sequence reads mapped to the ORF (Fig. 5A). To independently verify this outcome, we performed real-time PCR using total RNA templates from E12.5 littermate GFP-sorted cells not used for the RNA libraries (Fig. 5B). Direct comparison of the relative quantification (RQ) values for Exon1 vs. Exon2 ORF demonstrated



Gene Name	GFP/+ vs. GFP/GFP			GFP/GFP vs. <i>Ascl1KI/GFP</i>			Encoded protein, proposed function			
	GFP/+ RPKM Value	GFP/GFP RPKM Value	<i>Ascl1KI/GFP</i> RPKM Value	Log2 (Fold Change)	Adj. p-value	Q-value		Log2 (Fold Change)	Adj. p-value	Q-value
<i>Ascl1</i> **	7.4	14.9	15.7	1	5 X10 <sup>-5</sup>	0.01	0.11	NS	NS	Transcription factor, Neurogenesis
<i>Neurog2</i> **	30.2	35.5	112.3	0.3	NS	NS	1.6	5X10 <sup>-5</sup>	0.01	Transcription factor, Neurogenesis
<i>Atoh7</i> **	195.3	145	206	-0.4	0.01	NS	0.5	0.0009	NS	Transcription factor, RGC development
<i>Pou4f1</i> **	7.5	3.1	3.8	-1.5	5 X10 <sup>-5</sup>	0.01	0.3	NS	NS	Transcription factor, RGC development
<i>Pou4f2</i> **	53.1	30.5	70.9	-0.8	5X10 <sup>-5</sup>	0.01	1.2	5X10 <sup>-5</sup>	0.01	Transcription factor, RGC development
<i>Isl1</i> **	16.3	12.8	24.1	-0.4	NS	NS	0.63	0.01	NS	Transcription factor, Neurogenesis
<i>Onecut1</i>	0.76	1.1	5.1	0.6	NS	NS	0.4	NS	NS	Transcription factor, Cell Fate Determination
<i>Onecut2</i> **	16.6	7.7	25.3	-1	0.0002	0.04	0.7	5X10 <sup>-5</sup>	0.01	Transcription factor, Cell Fate Determination
<i>Onecut3</i>	3.8	1.2	1	-1.6	5X10 <sup>-5</sup>	0.01	-0.2	NS	NS	Transcription factor, Cell Fate Determination
<i>Ebf3</i>	28.9	11.6	18	-1.3	0.0001	0.02	0.6	NS	NS	Transcription factor, Differentiation
<i>Olig2</i> **	4.6	2.5	2.8	-0.9	0.0003	0.04	0.2	NS	NS	Transcription factor, Neurogenesis/Gliogenesis
<i>Neurod1</i> **	41.8	29	32.3	-0.5	0.02	NS	0.14	NS	NS	Transcription factor, Cell Differentiation
<i>Neurod4</i> **	18.3	9.4	15.1	-1	5X10 <sup>-5</sup>	0.01	0.7	5X10 <sup>-5</sup>	0.01	Transcription factor, Neural Development
<i>Notch3</i> **	5.4	5	8	-0.08	NS	NS	0.7	5X10 <sup>-5</sup>	0.01	Notch receptor, Signal Transduction
<i>Hes5</i> **	64.1	42.3	21.3	-0.6	0.001	NS	-1	5X10 <sup>-5</sup>	0.01	Transcription factor, Signal Transduction
<i>Hey1</i>	61.4	47	51.2	-0.4	0.009	NS	0.14	NS	NS	Transcription factor, Signal Transduction
<i>Dcc</i> **	53.8	32.6	37.8	-0.7	5X10 <sup>-5</sup>	0.01	0.23	NS	NS	Transmembrane protein, Axon Guidance
<i>Prdm1</i> #	17.8	10.7	11	-0.7	5X10 <sup>-5</sup>	0.01	0.05	NS	NS	Transcription factor, Differentiation
<i>Prdm13</i>	2.3	0.7	1.1	-1.7	5X10 <sup>-5</sup>	0.01	0.65	0.04	NS	Transcription factor, Differentiation
<i>Acsf6</i>	9.7	3.8	10.3	-1.3	0.0001	0.02	0.24	NS	NS	Acyl-CoA synthetase long-chain fam member 6
<i>Camk2n1</i>	24	13.9	22.9	-0.8	5X10 <sup>-5</sup>	0.01	0.7	5X10 <sup>-5</sup>	0.01	Calcium/calmodulin-dependent protein kinase II inhibitor 1
<i>Cd59a</i>	21.7	13.3	23.2	-0.7	0.0003	0.04	0.8	5X10 <sup>-5</sup>	0.01	Complement protein
<i>Gje1</i>	20.7	52	34	1.3	5X10 <sup>-5</sup>	0.01	-0.6	0.0003	0.04	Gap junction protein epsilon 1
<i>Insm2</i>	16.8	10.7	16	-0.6	0.0002	0.03	0.6	2.5 X10 <sup>-5</sup>	0.04	Insulinoma-associated protein
<i>Nova2</i>	12.7	6.1	9.9	-1	5X10 <sup>-5</sup>	0.01	0.7	5X10 <sup>-5</sup>	0.01	Neuro-oncological ventral antigen
<i>Nsg2</i>	16	7.6	11.8	-1.1	5X10 <sup>-5</sup>	0.01	0.7	0.0002	0.04	Neuron specific gene family member 2
<i>Rab3c</i>	2.6	1.3	2.2	-1	5X10 <sup>-5</sup>	0.01	0.7	0.0002	0.03	GTPase
<i>Tmem60</i>	42.4	74	29	0.8	5X10 <sup>-5</sup>	0.01	-1.3	5X10 <sup>-5</sup>	0.01	Transmembrane protein 60
<i>Trappc6b</i>	73	46	71	-0.7	5X10 <sup>-5</sup>	0.01	0.6	0.0002	0.03	Trafficking protein particle complex 6b

**Fig. 4.** Retinal development genes displaying significant expression changes among E12.5 *Neurog2*<sup>GFP/+</sup>, *Neurog2*<sup>GFP/GFP</sup>, and *Neurog2*<sup>Ascl1KI/GFP</sup> cells. Two selected alphabetical lists of genes with significant changes in gene expression. The first group contains those known to act during early retinogenesis; those in the second group are largely active in the CNS. Columns 2–4 are reads per kilobase of transcript per million mapped reads (RPKM) values. The log-fold changes between two different genotypes are listed in columns 5 and 8, followed by statistical significance in columns 6 and 9 = *P* values; columns 7 and 10 = *Q* values. Some transcripts had significant *Q* values in one genotypic comparison but not the other. Those genes validated by qPCR are denoted with \*\* or #. (# *Prdm1* validation can be found in Kowalchuk et al. 2018, in preparation). Three genes in the top group (gray shading) were significantly down-regulated in *Neurog2* mutants and up-regulated by ectopic *Ascl1*.

significantly elevated Exon1 transcript expression in *Neurog2*<sup>GFP/+</sup> and *Neurog2*<sup>Ascl1KI/GFP</sup> retinas, yet undetectable levels of the Exon2 ORF (Fig. 5B). We conclude that both mutant alleles are *Neurog2* nulls in the embryonic retina. Furthermore, biased distributions of *Neurog2* sequence reads containing 5' and 3' UTR segments obscured the lack of those for the protein-coding ORF.

Another gene predicted to be highly down-regulated in *Neurog2* mutants was *Atoh7*, given that it is a direct transcriptional target (Skowronska-Krawczyk et al., 2009). However, only a small, -0.4X-fold reduction was found (Fig. 4) (*P*=0.01). We attributed this to the developmental age of the starting material (E12.5). *Atoh7* expression levels were presumably even lower at the initiation of retinal neurogenesis (E11–E11.5), but in mutant cells isolated for sequencing, *Atoh7* transcription had probably begun to recover (Hufnagel et al., 2010). So we independently validated a significant down-regulation of *Atoh7* mRNA in *Neurog2*<sup>GFP/GFP</sup> eyes by qPCR (Fig. 6). Other bHLH factors also participate in aspects of RGC genesis, and subsets of *Atoh7*-lineage cells co-express *Neurod1* and/or *Neurod4/Math3* (Mao et al., 2008; Mao et al., 2013). Interestingly, the substitution of either gene into the *Atoh7* locus rescued RGC genesis (Mao et al., 2008; Mao et al., 2013). Yet another bHLH factor, *Olig2*, is expressed broadly by RPCs, although functions related to RGC neurogenesis have not been described (Nakamura et al., 2006; Shibasaki et al., 2007; Hafner et al., 2012). In other CNS tissues, *Olig2* specifies oligodendrocyte fates. All three factors, *Neurod1*, *Neurod4* and

*Olig2*, were significantly down-regulated in *Neurog2* mutants, with the latter two more severely affected (Fig. 4).

Work by multiple labs has elucidated a transcription factor hierarchy acting during vertebrate RGC development (reviewed in Centanin and Wittbrodt, 2014; Stenkamp, 2015). Here, *Atoh7* has been suggested to sit at a critical node. This is due to its early expression and phenotype, namely a total block of optic nerve formation and reduced expression of many genes in the early RGC network. Immediately downstream of *Atoh7* are the factors *Pou4f2* and *Isl1*, which act synergistically to cement the RGC fate (Mu et al., 2008; Pan et al., 2008; Li et al., 2014; Wu et al., 2015). Additional relevant RGC factors are *Pou4f1,3*, *Isl2*, *Onecut1,2,3*, *Myt1*, and *Ebf1,2,3*, which drive particular terminal differentiation processes or axonogenesis and/or specify functional subclasses of RGCs (Xiang et al., 1995; Erkman et al., 1996; Gan et al., 1999; Mu et al., 2008; Jin et al., 2010; Wu et al., 2012; Shi et al., 2013). Thus, it was not unexpected to find a highly significant reduction in transcript levels for *Pou4f1*, *Pou4f2*, *Onecut2*, *Onecut3*, and *Ebf3* in *Neurog2* mutants (Figs. 4 and 6). Although down-regulation of this entire set of early RGC regulators might be predicted, the transient nature of the *Neurog2* mutant phenotype, and cross-regulation among subsets of downstream factors, could effectively mask changes in particular genes. For example, while *Ebf1*, *Ebf2*, and *Ebf3* are all expressed by nascent RGCs, only *Ebf3* is a direct target of *Pou4f2* and was the sole *Ebf* paralogue significantly down-regulated here (Jin et al., 2010;

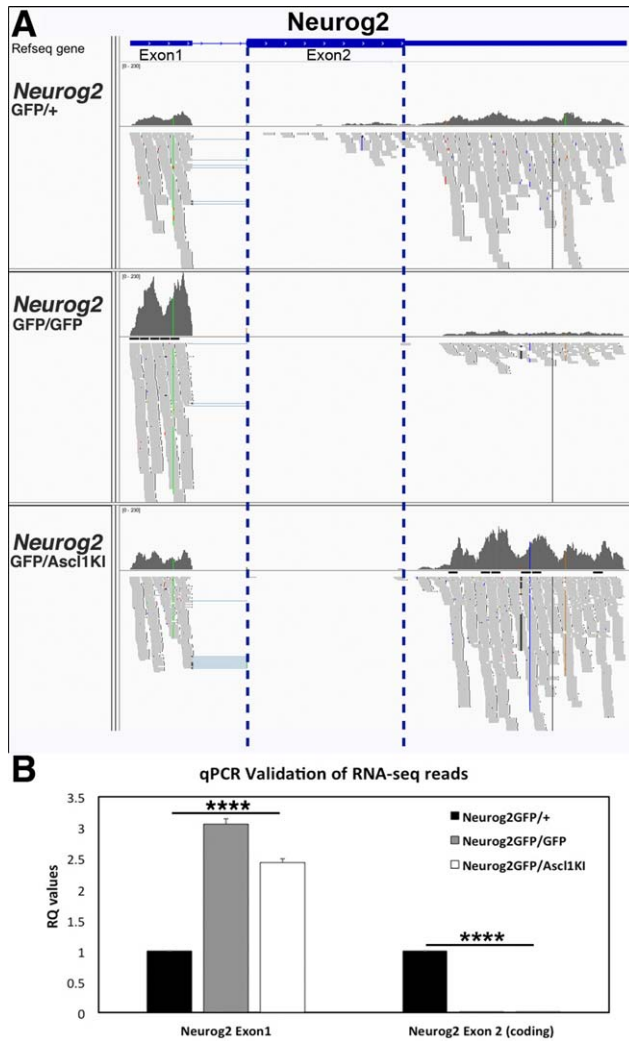


**Fig. 5.** *Neurog2* RNA-seq transcription profiles for gene-replacement mutations. IGV browser view of high-throughput sequences aligned to the *Neurog2* genomic locus (mm10). **A:** In all three genotypes, many reads mapped to 5' or 3' UTR. Blue dotted lines demarcate the ORF within Exon2 and better highlight the lack of sequence reads for both mutants. These alleles were made through precise replacement of *Neurog2* coding sequences with GFP or *Ascl1* cDNA, but retention of both endogenous UTRs (Fode et al., 2000; Seibt et al., 2003). **B:** Exon-specific qPCR using optic cup cDNA from E12.5 littermates of those used for RNA-seq libraries. Exon1 mRNA is elevated over control in both mutants, but both mutants lack Exon2-ORF mRNA.  $n = 3$  biologic replicates/genotype; \*\*\*\* $P \leq 0.0001$ ; error bars = SEM.

Gao et al., 2014) (Figs. (4 and 6)). We also noted a significant loss of the RGC axon-guidance molecule, *Dcc* (Figs. (4 and 6)) (Deiner et al., 1997; Livesey and Hunt, 1997). These data are consistent with *Neurog2* activity residing at the top of the early RGC genetic hierarchy.

### *Ascl1* Rescue Transcriptome

Another overt goal was to use transcriptomics to investigate the underlying basis of *Ascl1* rescue of the wave of neurogenesis in *Neurog2* mutants. Both *Neurog2*<sup>GFP/GFP</sup> and *Neurog2*<sup>Ascl1KI/GFP</sup> genotypes lacked functional *Neurog2* but also showed up-regulated endogenous *Ascl1* (Figs. 4–6). The specificity of the latter outcome was also validated by qPCR, using primers specific

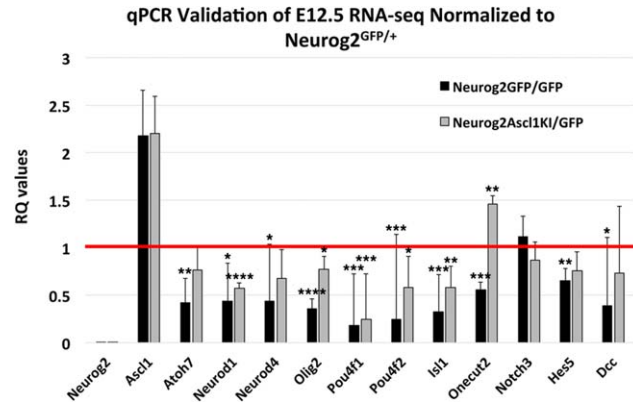


**Fig. 6.** Validation of gene-expression changes in a *Neurog2* allelic series. qPCR outcomes for 13 genes with significant  $Q$  and/or  $P$  values among the transcriptomic datasets. Elevated *Ascl1* levels solely reflect endogenous transcripts, since one primer resides in *Ascl1* 3'UTR that is not present in this replacement allele. *Neurog2*<sup>GFP/+</sup> cell transcript levels were normalized to 1. The *Neurog2* Exon2-ORF data from Figure 5B was also included here for comparison.  $n = 3$  biologic replicates/genotype; \* $P \leq 0.05$ ; \*\* $P \leq 0.01$ ; \*\*\* $P \leq 0.001$ ; \*\*\*\* $P \leq 0.0001$ ; error bars = SEM.

for an endogenous *Ascl1* gene amplicon (Fig. 6). Among the gene-expression lists with highly significant level changes ( $Q \leq 0.05$ ), we asked if there was a subset both down-regulated in *Neurog2* mutants and up-regulated in the *Ascl1* rescue. By these criteria, just three genes with known roles in developmental neurobiology were identified: *Neurod4*, *Pou4f2*, and *Onecut2* (gray shading in Fig. 4). We further confirmed these outcomes by qPCR, and also verified expression level changes for other factors with less robust but potentially meaningful alterations ( $P \leq 0.05$ ) (Figs. (4 and 6)). We also noted four bHLH factors, *Atoh7*, *Neurod1*, *Neurod4*, and *Olig2*, were each significantly increased in the *Neurog2*<sup>Ascl1KI/GFP</sup> GFP lineage, although none was restored to the level of *Neurog2* heterozygotes (Fig. 6). The simultaneous up-regulation of four bHLH factors was quite striking, particularly when combined with the up-regulation of *Pou4f2*, *Isl1*, and *Onecut2* (Fig. 6). Intriguingly, *Notch3* and *Hes5* levels were significantly altered in the *Neurog2*<sup>GFP/GFP</sup> vs. *Neurog2*<sup>Ascl1KI/GFP</sup> transcriptomes (Fig. 4), but only the changes in *Hes5* mRNA levels could be validated in a real-time PCR assay (Fig. 6). Overall, we conclude that the loss of *Neurog2* stalls retinal neurogenesis, thereby stimulating up-regulation of *Ascl1* to rescue RGC genesis within a lineage where it is otherwise not normally active.

## DISCUSSION

Retinal neurogenesis is a dynamic process that requires the coordination of multiple cellular activities. One intrinsic, temporal regulator of neurogenesis is the proneural bHLH transcription factor *Neurog2* (Hufnagel et al., 2010). Here we demonstrate that *Neurog2* simultaneously regulates RPC cell cycle exit and early RGC differentiation. Transcriptomic analyses confirmed that although *Neurog2* activity is required for *Atoh7* expression, it also impacted a broader transcription factor network underlying RGC development. We also found that ectopic *Ascl1* drove this same network to a sufficient threshold that correlates with a rescue of RGC development.

## Neurog2 Regulation of Cell Cycle Exit and Its Rescue by *Ascl1*

*Neurog2*-mutant RPCs do not exit mitosis appropriately, relative to controls. This is consistent with *Neurog2* promotion of cell cycle exit in the spinal cord and neuronal culture, where it stabilizes the cyclin-dependent kinase inhibitor *Cdkn1b/p27<sup>kip1</sup>* (Farah et al., 2000; Nguyen et al., 2006). By examining retinal cell cycle length via window labeling, we found an abnormal accumulation of mitotic RPCs in *Neurog2* mutants. We interpret this as a delay in cell cycle exit, since the proportion of S-phase RPCs is unaffected in E12.5 *Neurog2<sup>GFP/GFP</sup>* retinas (Hufnagel et al., 2010). We further propose that without *Neurog2*, RPCs accumulate at the G<sub>1</sub>/G<sub>0</sub> checkpoint. *Neurog2* regulation of *Cdkn1b* in other developmental contexts make it an appealing molecule to be affected here, and explain the delay in retinal neurogenesis. However, no significant changes in *Cdkn1b* mRNA levels were found in *Neurog2<sup>GFP/GFP</sup>* vs. *Neurog2<sup>GFP/+</sup>* transcriptomes. Nonetheless, loss of *Neurog2* might affect some other type of *Cdkn1b* regulation in the retina, and/or occur indirectly via *Atoh7*, since *Cdkn1b*+ cells are reduced in *Atoh7*-mutant retinas (Le et al., 2006). Regardless of which gene controls *Cdkn1b* expression, the regulation presumably occurs post-transcriptionally. It would be interesting to explore these mechanisms in the future, by testing for temporal retinogenesis phenotypes in *Cdkn1b* phosphorylation site-specific mutations (Besson et al., 2006).

The mechanism by which *Ascl1* misexpression rescued the cell cycle phenotype of *Neurog2*-mutant RPCs unfortunately remains unresolved. Throughout the nervous system, *Ascl1* was originally thought to promote cell cycle exit and neuronal differentiation (Ahmad et al., 1998; Cai et al., 2000; Tomita et al., 2000; Farah and Easter, 2005). Yet genomic profiling studies in the brain demonstrated that *Ascl1* can activate the expression of cell cycle progression genes, including canonical cell cycle regulators and oncogenic transcription factors (Castro et al., 2011). Although we overtly searched for up-regulated expression in these gene families, within the *Neurog2<sup>Ascl1KI/GFP</sup>* data set, no such candidates were identified. This would suggest that transcriptomic profiling to identify genes affected in temporal mutants may require tighter control of developmental time than is technically feasible during mouse embryogenesis.

## *Atoh7* as a Direct Downstream Target Gene for *Neurog2*

A key initiation step for retinal neurogenesis is *Neurog2* direct activation of *Atoh7* expression (Skowronska-Krawczyk et al., 2009). Lineage tracing and protein colocalization experiments show that in the embryonic retina, virtually all *Atoh7<sup>LacZ</sup>* cells are also *Neurog2*+, but not the reverse situation (Hufnagel et al., 2010; Miesfeld et al., 2018). Thus, at any given point, the *Neurog2* lineage should include more RPCs than the *Atoh7* lineage. Additionally, *Neurog2* and *Atoh7* are expressed during distinct cell cycle phases, with *Neurog2* largely found in mitotic cells and *Atoh7* predominantly present in postmitotic RPCs (Brown et al., 1998; Yang et al., 2003; Le et al., 2006; Ma and Wang, 2006; Brzezinski et al., 2012; Miesfeld et al., 2018). Together this suggests that a subset of *Neurog2*+ RPCs transit into *Atoh7*+ cells, complete cell cycle exit, and differentiate. The *Atoh7* mRNA expression domain was clearly smaller in E11.5 *Neurog2*-mutant retinas vs. controls (Hufnagel et al., 2010), implying there would

be a significant loss of *Atoh7* mRNA levels in mutant eyes. But this was not the case for the *Neurog2*-mutant transcriptome data set, although we did find a significant loss by qPCR. These differing outcomes might be attributed to variability in the precise age of the samples collected for each assay. Another confounding variable could be a more limited sequencing efficiency at the *Atoh7* locus due to high guanine-cytosine (GC) content. RNA-seq efficiency is reduced if GC content is either too high or too low (Risso et al., 2011; Zheng et al., 2011; Hansen et al., 2012; Filloux et al., 2014). The 5' end of the *Atoh7* transcript contains a 185 nucleotide stretch with ≥85% GC content (Prasov et al., 2010), which could introduce a negative bias for sequence read-depth.

## How Does *Ascl1* “Rescue” the *Neurog2* Temporal Phenotype?

In the developing mouse retina, *Ascl1* expression initiates about two days later than *Neurog2*, with its activity required for bipolar interneuron development and suppression of Müller glia (Jasoni and Reh, 1996; Tomita et al., 1996; Tomita et al., 2000; Brzezinski et al., 2011). Interestingly, the *Ascl1* lineage includes all major retinal cell classes except for RGCs, and the loss of *Ascl1* does not impact RGC differentiation. Yet one subset of *Ascl1*+ RPCs normally gives rise to *Atoh7*-expressing cells (Brzezinski et al., 2011). It is possible that in the *Neurog2*-mutant lineage ectopic *Ascl1* could directly activate *Atoh7* transcription given the multiple E-box binding sites (CANNTG) in conserved *Atoh7* regulatory DNA (Murre et al., 1989; Hutcheson et al., 2005; Hufnagel et al., 2007; Skowronska-Krawczyk et al., 2009). The binding specificity between bHLH factors relies largely on variations in the central NN nucleotides, but in particular contexts, sequences immediately surrounding the E-box are also influential (Powell et al., 2004; Seo et al., 2007; Gohlke et al., 2008; Gordan et al., 2013). In general, *Ascl1* has high affinity for CAGCTG consensus sequences, whereas *Neurog2* binds to CAGATC sequences (McNeill et al., 2012; Borromeo et al., 2014). Alternatively, we propose that rather than inappropriate binding of ectopic *Ascl1* to a preferred *Neurog2* consensus site, *Atoh7* transcription was prematurely stimulated via the same indirect regulatory mechanism normally employed within the endogenous *Ascl1* lineage (Brzezinski et al., 2011). Thus, the recovery of key genes in the RGC network in the *Neurog2<sup>Ascl1KI/GFP</sup>* data set could be attributed to *Ascl1* stimulation of *Atoh7* expression, which in turn activated the other genes. However, simultaneous up-regulation of four bHLH factors (along with *Pou4f2*, *Isl1* and *Onecut2*) suggests that ectopic *Ascl1* induced the transcription of multiple genes. *Ascl1* was previously shown to control genetic cascades, which give rise to particular neuronal fates in the brain, and maintain the right-size RPC pool for the late, postnatal retinal fates (Jasoni and Reh, 1996; Tomita et al., 1996; Tomita et al., 2000; Castro et al., 2011). *Ascl1* activity is also critical during retinal regeneration in multiple organisms (Wilken and Reh, 2016; Jorstad et al., 2017) and more recently implicated in mechanisms of tumorigenesis (Ma et al., 2017; Park et al., 2017). Thus, much more work is needed to tease apart the mode by which this factor successfully rescued RGC neurogenesis in the absence of *Neurog2*. Did *Ascl1* behave “normally” but in a new context to activate *Atoh7* or, by virtue of its interactions with chromatin remodeling proteins, rapidly stimulate the transcription of an array of genes above the minimum threshold necessary for RGC development?



TABLE 1. qPCR Primer Pairs

Gene	Primer 1	Primer 2
<i>Ascl1</i>	TTGAACTCTATGGCGGGTTC	CAAAGTCCATTCCCAGGAGA
<i>Atoh7</i>	ATCACCCCTACCTCCCTTTCC	CGAAGAGCCTCTGCCATA
<i>Dcc</i>	CAAGCTGGCTTTTGTACTCTTCG	GAACCTCTCGGTCGGACTCT
<i>Ebf3</i>	TCACCCTCCCTCAAACCTGTA	GTTTCACTGCGGAGATGACAT
<i>Hes5</i>	AGTCCCAAGGAGAAAAACCGA	GCTGTGTTTCAGGTAGCTGAC
<i>Gapdh</i>	TGAAGGGGTCGTTGATGG	AAAATGGTGAAGGTCGGTGT
<i>Isl1</i>	TATCCAGGGGATGACAGGAAC	GCTGTTGGGTGTATCTGGGAG
<i>Neurod1</i>	ATGACCAAATCATAACAGCGAGAG	TCTGCCTCGTGTTCCTCGT
<i>Neurod4</i>	AGCTGGTCCACACCACAATCCT	GTTCGAGCATTCCATAAGAGC
<i>Neurog2</i> exon1	AAGCAGCTCGGCTTTAACT	GTGTGTGTCGGGAATGT
<i>Neurog2</i> exon2	AACTCCACGTCCCATACAG	GAGGCGCATAACGATGCTTCT
<i>Notch3</i>	AAGCGTCTCCTGGATGCTG	GAATCTGGAAGACAGCCTGG
<i>Olig2</i>	TCCCCAGAACCCGATGATCTT	CGTGGACGAGGACGCAGTC
<i>Onecut1</i>	GGCAACGTGAGCGGTAGTTT	TTGCTGGGAGTTGTGAATGCT
<i>Onecut2</i>	AGAGGGTTCATGCCCCTCT	GGGATTTCTTCTGCGAGTTG
<i>Pou4f1</i>	AGGCCTATTTTGCCGTACAA	CGTCTCACACCCTCCTCAGT
<i>Pou4f2</i>	ATGGTGGTGGTGGCTCTTAC	CGGAGAGCTTGTCTTCCAAC
<i>Prdm1</i> Exon6	TGCTCACTACCCCAAGTTCC	TGGGATAAGCACCTCTTTGG
<i>Prdm1</i> 3'UTR	GAACCTGCTTTTCAAGTATGCTG	AGTGTAGACTTCACCGATGAGG
<i>Tubb3</i>	TAGACCCAGCGGCAACTAT	GTTCAGGTTCCAAGTCCACC

Finally, we propose that *Neurog2* also occupies the critical node for RGC development by virtue of its activation of *Atoh7*, plus other early bHLH factors. This is consistent with the significant down-regulation of *Pou4f1,2*, *Isl1*, *Onecut2*, and *Ebf3* in *Neurog2* mutants (Xiang et al., 1995; Erkman et al., 1996; Gan et al., 1999; Mu et al., 2008; Jin et al., 2010; Wu et al., 2012; Shi et al., 2013). Arguably, many of these same genes act downstream of and require *Atoh7*, but *Ascl1* substitutes only for *Neurog2*, and not *Atoh7* (Hufnagel et al., 2010; Hufnagel et al., 2013; Gao et al., 2014). Given that each bHLH factor has a “salt-and-pepper” pattern throughout retinogenesis, it provokes the question of how many bHLH factors an individual RPC must express at distinct time points, and whether particular combinations are sufficient to provide robustness for producing an RGC neuron. Although static co-expression pattern comparisons for all relevant transcription factors will be informative, we advocate single-cell genomics to gain the most accurate understanding of the complex and important question of which early factors drive RGC genesis.

## EXPERIMENTAL PROCEDURES

### Animals

Two gene-replacement allele mouse strains were used in this study: *Neurog2<sup>GFP</sup>* (*Neurog2<sup>tm4Fgu</sup>*) (Seibt et al., 2003) and *Neurog2<sup>Ascl1KI</sup>* (*Neurog2<sup>tm3(Ascl1)Fgu</sup>*) (Fode et al., 2000), both maintained on an ICR background. PCR genotyping was as previously described (Fode et al., 2000; Seibt et al., 2003). Embryonic age was determined through timed matings, with the date of the vaginal plug as E0.5. All mice were housed and cared for in accordance with the guidelines provided by the National Institutes of Health, Bethesda, Maryland, and the Association for Research in Vision and Ophthalmology, and conducted with

approval and oversight from the CCHRf and UC Davis Institutional Animal Care and Use Committees.

### Immunohistochemistry and Cell Quantification

Embryos were fixed in 4% paraformaldehyde/PBS (phosphate buffered saline) for 40–50 minutes at 4°C, cryoprotected in 5% and 15% sucrose/PBS, embedded in Tissue-Tek OCT, and 10- $\mu$ m cryosections immunolabeled as in Mastick and Andrews, 2001. Primary antibodies used were rat anti-BrdU (AbD Serotec, Cat #: OBT0030; 1:100), chick anti-GFP (Green Fluorescent Protein) (Abcam, AB13970; 1:1000), rabbit anti-Ki67 (Vector Labs, VP-K451; 1:1000), rabbit anti-PH3 (Millipore-Sigma, 06-570; 1:200), goat anti-Pou4f (Santa Cruz Biotechnology sc-6026; 1:50), and mouse anti-Isl1 IgG<sub>2B</sub> (Developmental Studies Hybridoma Bank, AB2314683; 1:50). Secondary antibodies were conjugated to Alexa Fluor 488 or Alexa Fluor 594 (Invitrogen/Life Science, Grand Island, NY; 1:500), or biotinylated (1:500) and sequentially labeled with streptavidin AMCA350 (Jackson ImmunoResearch, West Grove, PA; 1:200). Nuclear staining was performed with DAPI (1:1000 dilution of 10 mg/ml solution; Sigma, Cat #: 28718-90-3).

Microscopy was performed with either a ZEISS fluorescent microscope, ZEISS camera and Apotome deconvolution device, or Leica DM5500 microscope, equipped with a SPEI solid-state confocal. Images were processed using ZEISS AxioVision (v6.0), Leica LASAF, and/or Adobe Photoshop (CS4) software programs. All digital micrographs were equivalently adjusted for brightness, contrast, and pseudocoloring. Pou4f+GFP + or Isl1+GFP + cells were quantified using the count tool in Adobe Photoshop, CS4, and one-way ANOVA, plus a Bonferroni post hoc test used to determine *P* values (GraphPad Prism software, v6). In all experiments  $\geq 3$  individuals per genotype were analyzed, using at least 2 sections per individual. Equivalent anatomical depth in the retina was determined by proximity to the optic nerve.



## Mitotic Window Labeling

BrdU (5-Bromo-2'-deoxyuridine) was injected into pregnant dams (0.1 mg/g body weight of 10 mg/mL BrdU in 0.9 M NaCl) at either 1.5 hr or 18 hr prior to embryo harvest. For all analyses,  $\geq 3$  biologic replicate embryos per age and genotype were analyzed. Ten-micron cryosections were labeled as in Le et al., 2006, and BrdU+, Ki67+, and BrdU+Ki67+ populations quantified within the *Neurog2<sup>GFP</sup>* lineage, using the AxioVision measurements module. The percentage of GFP+BrdU+Ki67+ per GFP+BrdU+ cells  $\pm$  standard error of the mean (SEM) was calculated within a  $\times 100$  field, and one-way ANOVA plus Tukey's post hoc test used to determine *P* values (InStat Software, v3).

## Flow Cytometry and RNA Preparations

Pairs of E12.5 GFP+ optic cups were dissected and dissociated into single-cell suspensions using TrypLE Select (Invitrogen, 12563). The eBioscience 7-AAD viability marker (Thermo Fisher, 00-6993-50; 1:250) was added to all samples, and GFP+7AAD-neg cells purified with a Becton Dickinson FACS Aria machine. Total RNA was immediately extracted using the RNeasy Micro Kit (Qiagen, Cat #: 74004) and stored at  $-80^{\circ}\text{C}$ . All samples were submitted to the CCHR Gene Expression for quality assessment using an Agilent Bioanalyzer. Three biologic replicates per genotype were selected for RNA-seq analyses through a combination of matched somites counts, average total RNA concentration ( $\geq 1.97$  ng/ $\mu\text{l}$ ), and RIN (RNA Integrity Number) score ( $\geq 8.7$ ). The selected samples were then submitted for transcriptome analysis.

## RNA-seq and qPCR Analyses

Sequencing libraries were generated using the TruSeq RNA Library Prep Kit (Illumina, San Diego, CA, RS-122-2001) and analyzed on the Illumina Hi-Seq 2000 using single-end 50-bp read specifications with a read-depth of  $\geq 25$  million (Illumina). Following removal of primers and barcodes, sequence reads were aligned to the mm10 mouse genome assembly with the BWA and Bowtie programs. Aligned reads were analyzed for differentially expressed transcripts using the CuffDiff program in the Galaxy bioinformatics package ([www.usegalaxy.org](http://www.usegalaxy.org)). Differentially expressed transcripts were initially evaluated with an adjusted *P* value cutoff of  $Q \leq 0.05$ . For some transcripts, significance was broadened to  $P \leq 0.05$ , with the requirement of validation. Transcripts were grouped by ontology using PANTHER ([www.geneontology.org](http://www.geneontology.org)) and ranked by fold enrichment. The sequence reads (RPKM) for particular genes were visualized with the Integrative Genomics Viewer (IGV) browser (v.2.3) (Robinson et al., 2011; Thorvaldsdottir et al., 2013). RNA-seq data sets (see Supp. Tables 1,2) were deposited in NCBI Gene Expression Omnibus (Edgar et al., 2002) and assigned accession number GSE111666 (<https://www.ncbi.nlm.nih.gov/geo/query/acc.cgi?acc=GSE111666>).

Real-time PCR was performed by reverse transcribing E12.5 total retinal RNA into cDNA using SuperScript III (Thermo Fisher, 18080093) and performing qPCR with primer sets in Table 1, Fast SYBR Green Master Mix (Applied Biosystems, Cat #: 4385614), and an Applied Biosystems StepOnePlus machine. Relative quantification (RQ) values were calculated using the  $2^{-\Delta\Delta\text{CT}}$  method (Livak and Schmittgen, 2001) with GAPDH as endogenous control. Statistical significance was determined using IBM SPSS Statistics (v. 24) with an unpaired 2-sample *t*-test and Welch correction.

## ACKNOWLEDGMENTS

The authors thank Francois Guillemot for *Neurog2<sup>GFP/+</sup>* and *Neurog2<sup>Ascl1KI/+</sup>* mice; Maxime Mahe for sharing microdissection expertise and FAC-sorting protocols; Tina Liu for technical help; and the CCHMC Flow Cytometry, Gene Expression, and DNA Sequencing Cores for their services and guidance. We also thank the UC Davis eye development group for critical feedback and discussions; Richard Lang for use of a ZEISS Apotome imaging system; and Rebekah Karns (CCHMC) and Monica Britton (UC Davis) for guidance with bioinformatics analyses. This work was funded by Prevent Blindness Ohio-Young Female Investigator in Vision Research Fellowship Award to K.M.; NEI training grant T32 EY015387 to A.K.; and NIH/NEI R01 grant EY13612 to N.L.B.

## REFERENCES

- Ahmad I, Acharya HR, Rogers JA, Shibata A, Smithgall TE, Dooley CM. 1998. The role of NeuroD as a differentiation factor in the mammalian retina. *J Mol Neurosci* 11:165-178.
- Alexiades MR, Cepko C. 1996. Quantitative analysis of proliferation and cell cycle length during development of the rat retina. *Dev Dyn* 205:293-307.
- Besson A, Gurian-West M, Chen X, Kelly-Spratt KS, Kemp CJ, Roberts JM. 2006. A pathway in quiescent cells that controls p27Kip1 stability, subcellular localization, and tumor suppression. *Genes Dev* 20:47-64.
- Borromeo MD, Meredith DM, Castro DS, Chang JC, Tung KC, Guillemot F, Johnson JE. 2014. A transcription factor network specifying inhibitory versus excitatory neurons in the dorsal spinal cord. *Development* 141:2803-2812.
- Brown NL, Kanekar S, Vetter ML, Tucker PK, Gemza DL, Glaser T. 1998. Math5 encodes a murine basic helix-loop-helix transcription factor expressed during early stages of retinal neurogenesis. *Development* 125:4821-4833.
- Brown NL, Patel S, Brzezinski J, Glaser T. 2001. Math5 is required for retinal ganglion cell and optic nerve formation. *Development* 128:2497-2508.
- Brzezinski JA 4th, Kim EJ, Johnson JE, Reh TA. 2011. Ascl1 expression defines a subpopulation of lineage-restricted progenitors in the mammalian retina. *Development* 138:3519-3531.
- Brzezinski JA 4th, Prasov L, Glaser T. 2012. Math5 defines the ganglion cell competence state in a subpopulation of retinal progenitor cells exiting the cell cycle. *Dev Biol* 365:395-413.
- Cai L, Morrow EM, Cepko CL. 2000. Misexpression of basic helix-loop-helix genes in the murine cerebral cortex affects cell fate choices and neuronal survival. *Development* 127:3021-3030.
- Castro DS, Martynoga B, Parras C, Ramesh V, Pacary E, Johnston C, Drechsel D, Lebel-Potter M, Garcia LG, Hunt C, Dolle D, Bithell A, Ettwiller L, Buckley N, Guillemot F. 2011. A novel function of the proneural factor Ascl1 in progenitor proliferation identified by genome-wide characterization of its targets. *Genes Dev* 25:930-945.
- Centanin L, Wittbrodt J. 2014. Retinal neurogenesis. *Development* 141:241-244.
- Chenn A, Walsh CA. 2002. Regulation of cerebral cortical size by control of cell cycle exit in neural precursors. *Science* 297:365-369.
- Deiner MS, Kennedy TE, Fazeli A, Serafini T, Tessier-Lavigne M, Sretavan DW. 1997. Netrin-1 and DCC mediate axon guidance locally at the optic disc: loss of function leads to optic nerve hypoplasia. *Neuron* 19:575-589.
- Edgar R, Domrachev M, Lash AE. 2002. *Nucleic Acids Research* 30: 207-10.
- Erkman L, McEvelly RJ, Luo L, Ryan AK, Hooshmand F, O'Connell SM, Keithley EM, Rapaport DH, Ryan AF, Rosenfeld MG. 1996. Role of transcription factors Brn-3.1 and Brn-3.2 in auditory and visual system development. *Nature* 381:603-606.
- Farah MH, Easter SS Jr. 2005. Cell birth and death in the mouse retinal ganglion cell layer. *J Comp Neurol* 489:120-134.
- Farah MH, Olson JM, Susic HB, Hume RI, Tapscott SJ, Turner DL. 2000. Generation of neurons by transient expression of neural bHLH proteins in mammalian cells. *Development* 127:693-702.

- Feng L, Xie ZH, Ding Q, Xie X, Libby RT, Gan L. 2010. MATH5 controls the acquisition of multiple retinal cell fates. *Mol Brain* 3:36.
- Filloux C, Meersseman C, Philippe R, Forestier L, Klopp C, Rocha D, Maftah A, Petit D. 2014. An integrative method to normalize RNA-Seq data. *BMC Bioinformatics* 15:188.
- Fode C, Gradwohl G, Morin X, Dierich A, LeMeur M, Goridis C, Guillemot F. 1998. The bHLH protein NEUROGENIN 2 is a determination factor for epibranchial placode-derived sensory neurons. *Neuron* 20:483–494.
- Fode C, Ma Q, Casarosa S, Ang SL, Anderson DJ, Guillemot F. 2000. A role for neural determination genes in specifying the dorsoventral identity of telencephalic neurons. *Genes Dev* 14:67–80.
- Gan L, Wang SW, Huang Z, Klein WH. 1999. POU domain factor Brn-3b is essential for retinal ganglion cell differentiation and survival but not for initial cell fate specification. *Dev Biol* 210:469–480.
- Gan L, Xiang M, Zhou L, Wagner DS, Klein WH, Nathans J. 1996. POU domain factor Brn-3b is required for the development of a large set of retinal ganglion cells. *Proc Natl Acad Sci U S A* 93:3920–3925.
- Gao Z, Mao CA, Pan P, Mu X, Klein WH. 2014. Transcriptome of Atoh7 retinal progenitor cells identifies new Atoh7-dependent regulatory genes for retinal ganglion cell formation. *Dev Neurobiol* 74:1123–1140.
- Gohlke JM, Armant O, Parham FM, Smith MV, Zimmer C, Castro DS, Nguyen L, Parker JS, Gradwohl G, Portier CJ, Guillemot F. 2008. Characterization of the proneural gene regulatory network during mouse telencephalon development. *BMC Biol* 6:15.
- Gordan R, Shen N, Dror I, Zhou T, Horton J, Rohs R, Bulyk ML. 2013. Genomic regions flanking E-box binding sites influence DNA binding specificity of bHLH transcription factors through DNA shape. *Cell Rep* 3:1093–1104.
- Gradwohl G, Fode C, Guillemot F. 1996. Restricted expression of a novel murine atonal-related bHLH protein in undifferentiated neural precursors. *Dev Biol* 180:227–241.
- Hafler BP, Surzenko N, Beier KT, Punzo C, Trimarchi JM, Kong JH, Cepko CL. 2012. Transcription factor Olig2 defines subpopulations of retinal progenitor cells biased toward specific cell fates. *Proc Natl Acad Sci U S A* 109:7882–7887.
- Hansen KD, Irizarry RA, Wu Z. 2012. Removing technical variability in RNA-seq data using conditional quantile normalization. *Biostatistics* 13:204–216.
- Hu M, Easter SS. 1999. Retinal neurogenesis: the formation of the initial central patch of postmitotic cells. *Dev Biol* 207:309–321.
- Hufnagel RB, Le TT, Riesenber AL, Brown NL. 2010. Neurog2 controls the leading edge of neurogenesis in the mammalian retina. *Dev Biol* 340:490–503.
- Hufnagel RB, Riesenber AN, Quinn M, Brzezinski JA 4th, Glaser T, Brown NL. 2013. Heterochronic misexpression of *Ascl1* in the Atoh7 retinal cell lineage blocks cell cycle exit. *Mol Cell Neurosci* 54:108–120.
- Hufnagel RB, Riesenber AN, Saul SM, Brown NL. 2007. Conserved regulation of *Math5* and *Math1* revealed by *Math5*-GFP transgenes. *Mol Cell Neurosci* 36:435–448.
- Hutcheson DA, Hanson MI, Moore KB, Le TT, Brown NL, Vetter ML. 2005. bHLH-dependent and -independent modes of *Ath5* gene regulation during retinal development. *Development* 132:829–839.
- Jasoni CL, Reh TA. 1996. Temporal and spatial pattern of MASH-1 expression in the developing rat retina demonstrates progenitor cell heterogeneity. *J Comp Neurol* 369:319–327.
- Jin K, Jiang H, Mo Z, Xiang M. 2010. Early B-cell factors are required for specifying multiple retinal cell types and subtypes from postmitotic precursors. *J Neurosci* 30:11902–11916.
- Jorstad NL, Wilken MS, Grimes WN, Wohl SG, VandenBosch LS, Yoshimatsu T, Wong RO, Rieke F, Reh TA. 2017. Stimulation of functional neuronal regeneration from Muller glia in adult mice. *Nature* 548:103–107.
- Kee N, Sivalingam S, Boonstra R, Wojtowicz JM. 2002. The utility of Ki-67 and BrdU as proliferative markers of adult neurogenesis. *J Neurosci Methods* 115:97–105.
- Le TT, Wroblewski E, Patel S, Riesenber AN, Brown NL. 2006. *Math5* is required for both early retinal neuron differentiation and cell cycle progression. *Dev Biol* 295:764–778.
- Li R, Wu F, Ruonala R, Sapkota D, Hu Z, Mu X. 2014. *Isl1* and *Pou4f2* form a complex to regulate target genes in developing retinal ganglion cells. *PLoS One* 9:e92105.
- Livak KJ, Schmittgen TD. 2001. Analysis of relative gene expression data using real-time quantitative PCR and the 2(-Delta Delta C(T)) Method. *Methods* 25:402–408.
- Livesey FJ, Hunt SP. 1997. Netrin and netrin receptor expression in the embryonic mammalian nervous system suggests roles in retinal, striatal, nigral, and cerebellar development. *Mol Cell Neurosci* 8:417–429.
- Ma H, Du X, Zhang S, Wang Q, Yin Y, Qiu X, Da P, Yue H, Wu H, Xu F. 2017. Achaete-scute complex homologue-1 promotes development of laryngocarcinoma via facilitating the epithelial-mesenchymal transformation. *Tumour Biol* 39:1010428317705752.
- Ma W, Wang SZ. 2006. The final fates of neurogenin2-expressing cells include all major neuron types in the mouse retina. *Mol Cell Neurosci* 31:463–469.
- Mao CA, Cho JH, Wang J, Gao Z, Pan P, Tsai WW, Frishman LJ, Klein WH. 2013. Reprogramming amacrine and photoreceptor progenitors into retinal ganglion cells by replacing *Neurod1* with *Atoh7*. *Development* 140:541–551.
- Mao CA, Wang SW, Pan P, Klein WH. 2008. Rewiring the retinal ganglion cell gene regulatory network: *Neurod1* promotes retinal ganglion cell fate in the absence of *Math5*. *Development* 135:3379–3388.
- Mastick GS, Andrews GL. 2001. *Pax6* regulates the identity of embryonic diencephalic neurons. *Mol Cell Neurosci* 17:190–207.
- McCabe KL, Gunther EC, Reh TA. 1999. The development of the pattern of retinal ganglion cells in the chick retina: mechanisms that control differentiation. *Development* 126:5713–5724.
- McNeill B, Perez-Iratxeta C, Mazerolle C, Furimsky M, Mishina Y, Andrade-Navarro MA, Wallace VA. 2012. Comparative genomics identification of a novel set of temporally regulated hedgehog target genes in the retina. *Mol Cell Neurosci* 49:333–340.
- Miesfeld JB, Glaser T, Brown NL. 2018. The dynamics of native Atoh7 protein expression during mouse retinal histogenesis, revealed with a new antibody. *Gene Expr Patterns* 27:114–121.
- Mu X, Fu X, Beremand PD, Thomas TL, Klein WH. 2008. Gene regulation logic in retinal ganglion cell development: *Isl1* defines a critical branch distinct from but overlapping with *Pou4f2*. *Proc Natl Acad Sci U S A* 105:6942–6947.
- Murre C, McCaw PS, Vaessin H, Caudy M, Jan LY, Jan YN, Cabrera CV, Buskin JN, Hauschka SD, Lassar AB, et al. 1989. Interactions between heterologous helix-loop-helix proteins generate complexes that bind specifically to a common DNA sequence. *Cell* 58:537–544.
- Nakamura K, Harada C, Namekata K, Harada T. 2006. Expression of *olig2* in retinal progenitor cells. *Neuroreport* 17:345–349.
- Nguyen L, Besson A, Heng JI, Schuurmans C, Teboul L, Parras C, Philpott A, Roberts JM, Guillemot F. 2006. *p27kip1* independently promotes neuronal differentiation and migration in the cerebral cortex. *Genes Dev* 20:1511–1524.
- Pan L, Deng M, Xie X, Gan L. 2008. *ISL1* and *BRN3B* co-regulate the differentiation of murine retinal ganglion cells. *Development* 135:1981–1990.
- Park NI, Guilhamon P, Desai K, McAdam RF, Langille E, O'Connor M, Lan X, Whetstone H, Coutinho FJ, Vanner RJ, Ling E, Prinos P, Lee L, Selvadurai H, Atwal G, Kushida M, Clarke ID, Voisin V, Cusimano MD, Bernstein M, Das S, Bader G, Arrowsmith CH, Angers S, Huang X, Lupien M, Dirks PB. 2017. *ASCL1* Reorganizes Chromatin to Direct Neuronal Fate and Suppress Tumorigenicity of Glioblastoma Stem Cells. *Cell Stem Cell* 21:209–224 e207.
- Pei Z, Wang B, Chen G, Nagao M, Nakafuku M, Campbell K. 2011. Homeobox genes *Gsx1* and *Gsx2* differentially regulate telencephalic progenitor maturation. *Proc Natl Acad Sci U S A* 108:1675–1680.
- Powell LM, Zur Lage PI, Prentice DR, Senthinathan B, Jarman AP. 2004. The proneural proteins *Atonal* and *Scute* regulate neural target genes through different E-box binding sites. *Mol Cell Biol* 24:9517–9526.
- Prada C, Puga J, Perez-Mendez L, Lopez, Ramirez G. 1991. Spatial and Temporal Patterns of Neurogenesis in the Chick Retina. *Eur J Neurosci* 3:1187.

- Prasov L, Brown NL, Glaser T. 2010. A critical analysis of Atoh7 (Math5) mRNA splicing in the developing mouse retina. *PLoS One* 5:e12315.
- Rapaport DH, Wong LL, Wood ED, Yasumura D, LaVail MM. 2004. Timing and topography of cell genesis in the rat retina. *J Comp Neurol* 474:304–324.
- Repka AM, Adler R. 1992. Accurate determination of the time of cell birth using a sequential labeling technique with [3H]-thymidine and bromodeoxyuridine (“window labeling”). *J Histochem Cytochem* 40:947–953.
- Riesenberg AN, Le TT, Willardsen MI, Blackburn DC, Vetter ML, Brown NL. 2009. Pax6 regulation of Math5 during mouse retinal neurogenesis. *Genesis* 47:175–187.
- Risso D, Schwartz K, Sherlock G, Dudoit S. 2011. GC-content normalization for RNA-Seq data. *BMC Bioinformatics* 12:480.
- Robinson JT, Thorvaldsdottir H, Winckler W, Guttman M, Lander ES, Getz G, Mesirov JP. 2011. Integrative genomics viewer. *Nat Biotechnol* 29:24–26.
- Seibt J, Schuurmans C, Gradwohl G, Dehay C, Vanderhaeghen P, Guillemot F, Polleux F. 2003. Neurogenin2 specifies the connectivity of thalamic neurons by controlling axon responsiveness to intermediate target cues. *Neuron* 39:439–452.
- Seo S, Lim JW, Yellajoshiyula D, Chang LW, Kroll KL. 2007. Neurogenin and NeuroD direct transcriptional targets and their regulatory enhancers. *EMBO J* 26:5093–5108.
- Shi M, Kumar SR, Motajo O, Kretschmer F, Mu X, Badea TC. 2013. Genetic interactions between Brn3 transcription factors in retinal ganglion cell type specification. *PLoS One* 8:e76347.
- Shibasaki K, Takebayashi H, Ikenaka K, Feng L, Gan L. 2007. Expression of the basic helix-loop-factor Olig2 in the developing retina: Olig2 as a new marker for retinal progenitors and late-born cells. *Gene Expr Patterns* 7:57–65.
- Sidman RL. 1961. Histogenesis of mouse retina studied with thymidine-H3. In: Smelser GK, editor. *The Structure of the Eye*. New York: Academic Press. p 487–506.
- Skowronska-Krawczyk D, Chiodini F, Ebeling M, Alliod C, Kundzewicz A, Castro D, Ballivet M, Guillemot F, Matter-Sadzinski L, Matter JM. 2009. Conserved regulatory sequences in Atoh7 mediate non-conserved regulatory responses in retina ontogenesis. *Development* 136:3767–3777.
- Sommer L, Ma Q, Anderson DJ. 1996. Neurogenins, a novel family of atonal-related bHLH transcription factors, are putative mammalian neuronal determination genes that reveal progenitor cell heterogeneity in the developing CNS and PNS. *Mol Cell Neurosci* 8:221–241.
- Stenkamp DL. 2015. Development of the Vertebrate Eye and Retina. *Prog Mol Biol Transl Sci* 134:397–414.
- Thorvaldsdottir H, Robinson JT, Mesirov JP. 2013. Integrative Genomics Viewer (IGV): high-performance genomics data visualization and exploration. *Brief Bioinform* 14:178–192.
- Tomita K, Moriyoshi K, Nakanishi S, Guillemot F, Kageyama R. 2000. Mammalian achaete-scute and atonal homologs regulate neuronal versus glial fate determination in the central nervous system. *EMBO J* 19:5460–5472.
- Tomita K, Nakanishi S, Guillemot F, Kageyama R. 1996. Mash1 promotes neuronal differentiation in the retina. *Genes Cells* 1:765–774.
- Turner DL, Cepko CL. 1987. A common progenitor for neurons and glia persists in rat retina late in development. *Nature* 328:131–136.
- Turner DL, Snyder EY, Cepko CL. 1990. Lineage-independent determination of cell type in the embryonic mouse retina. *Neuron* 4:833–845.
- Wang SW, Kim BS, Ding K, Wang H, Sun D, Johnson RL, Klein WH, Gan L. 2001. Requirement for math5 in the development of retinal ganglion cells. *Genes Dev* 15:24–29.
- Wilken MS, Reh TA. 2016. Retinal regeneration in birds and mice. *Curr Opin Genet Dev* 40:57–64.
- Wu F, Kaczynski TJ, Sethuramanujam S, Li R, Jain V, Slaughter M, Mu X. 2015. Two transcription factors, Pou4f2 and Isl1, are sufficient to specify the retinal ganglion cell fate. *Proc Natl Acad Sci U S A* 112:E1559–1568.
- Wu F, Sapkota D, Li R, Mu X. 2012. Onecut 1 and Onecut 2 are potential regulators of mouse retinal development. *J Comp Neurol* 520:952–969.
- Xiang M, Zhou L, Macke JP, Yoshioka T, Hendry SH, Eddy RL, Shows TB, Nathans J. 1995. The Brn-3 family of POU-domain factors: primary structure, binding specificity, and expression in subsets of retinal ganglion cells and somatosensory neurons. *J Neurosci* 15:4762–4785.
- Yan RT, Ma WX, Wang SZ. 2001. neurogenin2 elicits the genesis of retinal neurons from cultures of nonneural cells. *Proc Natl Acad Sci U S A* 98:15014–15019.
- Yang Z, Ding K, Pan L, Deng M, Gan L. 2003. Math5 determines the competence state of retinal ganglion cell progenitors. *Dev Biol* 264:240–254.
- Young RW. 1985. Cell differentiation in the retina of the mouse. *Anat Rec* 212:199–205.
- Zheng W, Chung LM, Zhao H. 2011. Bias detection and correction in RNA-Sequencing data. *BMC Bioinformatics* 12:290.